



## Coordination of Ti cation embedded in argon clusters

Michalis Velegrakis<sup>a,\*</sup>, George E. Froudakis<sup>a,b</sup>, Stavros C. Farantos<sup>a,b</sup>

<sup>a</sup> *Institute of Electronic Structure and Laser, Foundation for Research and Technology – Hellas, P.O. Box 1527, 711 10 Heraklion, Crete, Greece*

<sup>b</sup> *Department of Chemistry, University of Crete, 711 10 Heraklion, Crete, Greece*

Received 15 December 1998; in final form 12 January 1999

### Abstract

A laser vaporisation source and a time-of-flight mass spectrometer are used for the production and detection of  $\text{Ti}^+\text{Ar}_n$  clusters. Parallel, density functional theory (DFT) calculations assist in extracting the structures of the first members of the series. The mass spectrum is dominated by one intense line of  $\text{Ti}^+\text{Ar}_6$ , for which the DFT calculations predict a regular octahedron. © 1999 Elsevier Science B.V. All rights reserved.

### 1. Introduction

Metal-doped noble gas clusters of the type  $\text{MX}_n$  ( $\text{M}$  = metal and  $\text{X}$  = noble gas atom) constitute prototype systems in modelling metal–ligand interactions, ranging from the gas-phase diatomic complexes up to the bulk phase. Therefore, studies on these systems have evolved to a topic of considerable interest [1–3]. If the metal exhibits a  $s$  orbital electronic configuration, the noble gas atoms tend to arrange around the central metal core. In this case, the cluster structure is often dictated by geometrical factors such as the atomic radii ratio of the metal and ligand. Such arrangements have often been observed in the mass spectra of  $\text{MX}_n$  cluster systems [4–7] and have also been successfully explained [6–9].

The situation is substantially different if the metal is a transition metal. Here, the transition element is an open-shell system and forces the noble gas atoms

to occupy certain sites depending on the filled or empty  $d$ -orbitals. This has been documented in mass spectrometric work [10–14] for a series of transition metal ions exhibiting a  $d^k$  electronic configuration. Using arguments adopted from ligand field theory (LFT), it was possible to predict the stability and the structure of some transition metal ion-doped noble gas clusters. However, for transition metal ions, whose lower electronic state is of the  $d^{k-1}s^1$  kind, a number of nearly degenerate low-lying electronic states exist. Furthermore, in the complexes of these ions with atomic or molecular ligands, mixing of these states is expected and therefore the application of simple LFT arguments in predicting the structure and the stability of these clusters is not straightforward.

Partridge et al. [15,16] have performed extended ab initio calculations for the spectroscopic constants of the ground and some low-lying electronic states for all of the first-row transition metal cations with He, Ne and Ar. These studies have shown that the interaction forces are predominately electrostatic, i.e. charge-induced dipole interactions. For metal ions

\* Corresponding author. Fax: +30 81 391318; e-mail: vele@iesl.forth.gr

with a  $3d^{k-1}4s^1$  electronic configuration, the attractive forces are additionally enhanced either through hybridisation or eventually  $4s$  to  $3d$  promotion. In this sense, the case of  $Ti^+$  is of particular interest as its first electronic excited state is  $3d^34s^0$  ( $^4F$ ) and is separated from the ground state  $3d^24s^1$  ( $^4F$ ) by only 0.11 eV. The small energy difference of the electronic states results in the mixing these two states in the  $Ti^+$ –noble gas diatomic complexes, a phenomenon which becomes more pronounced as one goes from He to Ar [16].

Ligand-induced configuration mixing has been also observed in the  $Ti^+$ -doped molecular clusters  $Ti^+(CH_4)_n$  [17], and  $Ti^+(H_2)_n$  [18]. The thorough experimental and theoretical results of Bushnell et al. [18] for  $Ti^+(H_2)_n$  clusters have shown that as the number of ligands increases the electronic ground state of the cation changes completely from  $3d^24s^1$  to  $3d^34s^0$ . This crossing occurs for the case of  $Ti^+(CH_4)_n$  after the addition of three  $CH_4$  molecules, while for  $Ti^+(H_2)_n$  only one  $H_2$  is needed to change the electronic configuration of  $Ti^+$ .

Knight et al. [19] have performed electron–spin resonance studies on  $Ti^+$  isolated in neon and argon gas matrices. Due to the very small hyperfine splitting observed in these experiments, they suggested a  $3d^3$  electronic configuration for the Ti cation surrounded by an octahedral matrix environment. These results indicate that by the addition of six noble gas atoms the  $Ti^+$  ground state may have been completely changed from  $3d^24s^1$  to  $3d^34s^0$ .

The purpose of the present Letter is to investigate the structures of the first small aggregates of  $Ti^+Ar_n$ . For this, we have recorded time-of-flight (TOF) spectra for the clusters of titanium with argon. Parallel ab initio calculations for the small members of the series assist in deducing the most stable structures and the geometrical parameters of these complexes.

## 2. Experimental and theoretical methods

The molecular beam apparatus used to carry out the experiments consists of three differentially pumped chambers and it is equipped with a TOF mass spectrometer. This system is described in detail elsewhere [4,5]. Briefly, the metal ion-doped Ar clusters are formed in a laser vapourisation source,

where a pulsed infrared Nd:YAG laser produces plasma from a pure Ti target. The plasma plume is mixed with an expanding Ar gas pulse provided by a home-built nozzle. The adiabatic expansion results in cooling of the nascent clusters, thus forming a cluster beam, which contains neutral clusters as well as ionic species. We study the positive ions, which are produced directly from the plasma/noble gas mixing without the use of post-ionization. Hence, it is expected that these clusters are sufficiently relaxed, and the measured size distribution reflects the stability of these species. After passing a skimmer, the ions are accelerated by a pulsed two-field TOF apparatus and focused into a microchannel plate detector where the TOF mass spectra can be recorded with a computer-controlled digital storage oscilloscope.

The theoretical treatment of the transition metal ion-doped argon aggregates involved density functional theory (DFT) calculations with the Gaussian 94 program package [20]. The three-parameter hybrid functional of Becke [21] using the Lee–Yang–Parr correlation functional [22] (B3LYP), was employed for the geometry optimizations. The atomic basis set that we use include Gaussian functions of triple-zeta quality augmented by d-polarization functions ( $6-311G^*$ ) [20].

## 3. Results and discussion

Fig. 1 displays the TOF spectra for  $Ti^+$ -doped Ar clusters. The spectrum represents the average result over 1000 laser shots and is reproducible, indepen-

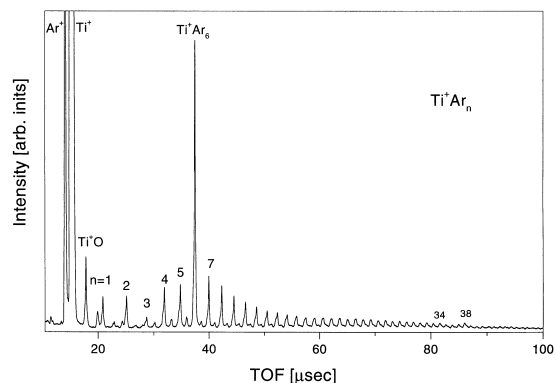


Fig. 1. Time-of-flight spectra of the  $Ti^+Ar_n$  clusters. The labels indicate the number of  $n$  of Ar atoms.

dent of the formation conditions (backing pressure, laser fluence, etc.). The small peaks between the main  $\text{Ti}^+\text{Ar}_n$  clusters series correspond to  $(\text{TiO})^+\text{Ar}_n$  and to  $(\text{TiH}_2\text{O})^+\text{Ar}_n$  clusters originating from water impurities in the Ar gas inlet line. The range of the cluster sizes observed extends up to  $n = 50$ . No magic numbers sequences can be observed clearly in the spectrum, except the very pronounced peak which corresponds to the  $\text{Ti}^+\text{Ar}_6$  complex, the smaller intensity of the  $n = 3$  cluster and some irregularities at  $n = 34$  and  $n = 39$ .

It should be noted that the peak at  $n = 6$  dominates in the spectrum independently of the mass spectroscopic conditions.

In order to investigate the stability of the small  $\text{Ti}^+\text{Ar}_n$  ( $n = 1-7$ ) clusters, we performed first-principles calculations for the minimum energy structures. All the structures presented here are optimized at the DFT/6-311G\* level. Various initial geometries were tested for each cluster. The lowest-energy structures that we obtained are presented in Fig. 2, while the total energy  $E_{\text{tot}}$ , the binding energies

$$E(n) = E_{\text{tot}} - E(\text{Ti}^+) - nE(\text{Ar}),$$

of these structures and the charge on Ti (obtained from a Mulliken population analysis) are listed in Table 1.

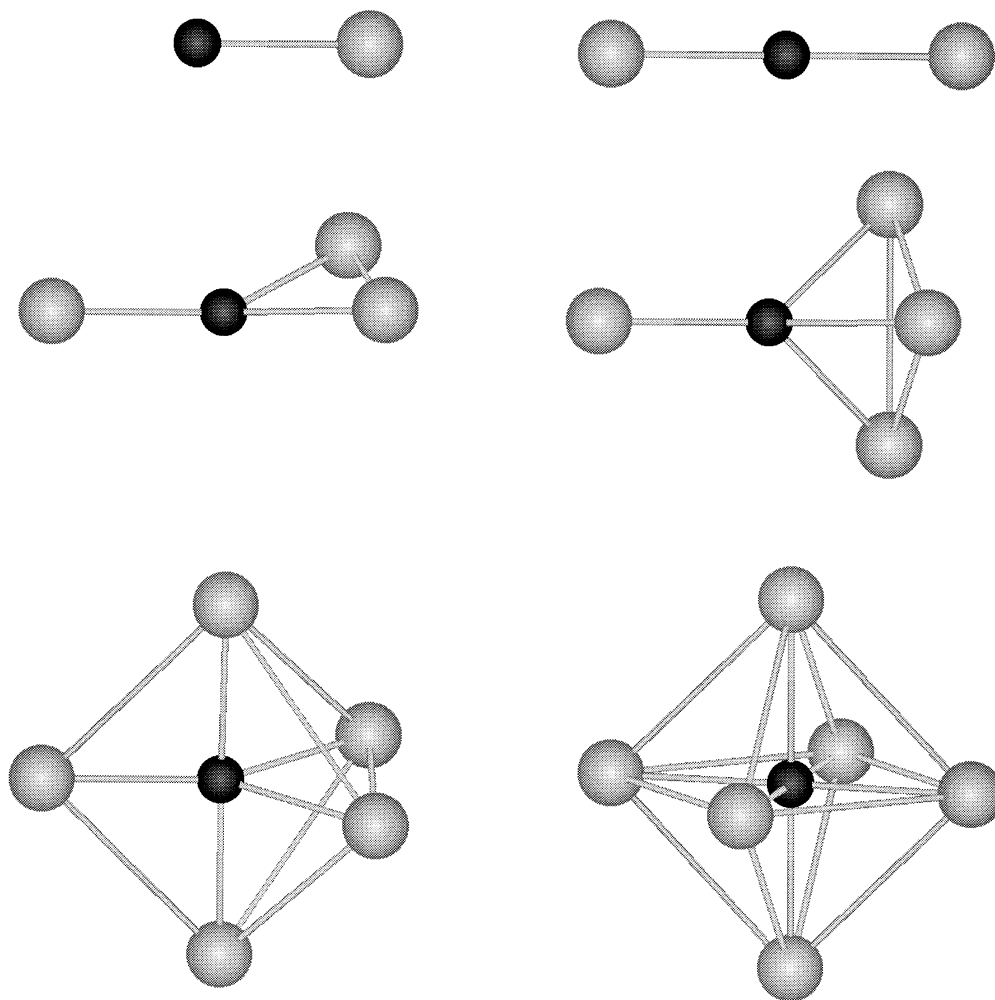


Fig. 2. Ground state geometries of the  $\text{Ti}^+\text{Ar}_n$  ( $n = 1-6$ ) clusters, obtained by DFT.

Table 1

Total energies, binding energies and charge on the Ti atom obtained at the B3LYP/6-311G\* level of theory

$n$	Total energy (hartree)	Binding energy (eV)	Mulliken populations Ti
0	-849.0981		
1	-1376.65997	0.236	0.92
2	-1904.22294	0.501	0.84
3	-2431.77751	0.538	0.82
4	-2959.33165	0.564	0.76
5	-3486.88621	0.6	0.78
6	-4014.44145	0.655	0.76
7	-4541.99458	0.653	

As previously mentioned, the bonding in the  $\text{Ti}^+\text{Ar}$  dimer arises from a mixture of the  $3d^3$  and  $3d^24s^1$  configurations [16]. Therefore, calculations on such systems employing single-reference methods should be interpreted with caution. However, Bushnell et al. [18] have shown that the geometrical properties and the relative energies of  $\text{Ti}^+(\text{H}_2)_{1,2}$  complexes obtained by employing the DFT method are in good agreement with those of multireference methods. Furthermore, DFT has provided reasonable results for the ground states of some transition metal–noble gas [12,14] or molecular [17,18] clusters. Therefore, the use of the DFT method to study large clusters such as  $\text{Ti}^+\text{Ar}_n$ ,  $n < 8$ , is reasonable. For the diatomic  $\text{Ti}^+\text{Ar}$  complex, we found a bonding distance of 2.65 Å and a binding energy of 0.24 eV. These results are in good agreement with those reported by Partridge and Bauschlicher [16] (bond length 2.65 Å and binding energy 0.3 eV) using a multireference method (ICMRCI + Q).

As can be seen in Fig. 2, the geometry of  $\text{Ti}^+\text{Ar}_2$  is a linear structure with two Ti–Ar bonds of 2.65 Å. In the case of  $\text{Ti}^+\text{Ar}_3$ , the most stable geometry is a trigonal pyramid with one short Ti–Ar bond (2.65 Å) and two longer bonds of 2.88 Å. The structure of  $\text{Ti}^+\text{Ar}_4$  is a distorted tetrahedron, where the Ar atoms are placed at the vertexes and the  $\text{Ti}^+$  occupies the central position. Again there are one short Ti–Ar bond of 2.66 Å and three longer bonds of  $\sim 3$  Å.  $\text{Ti}^+\text{Ar}_5$  cluster is a trigonal bipyramid and again one Ti–Ar bond is shorter (2.73 Å), as compared with the bond length ( $\sim 2.9$  Å) of the four others. Finally, in  $\text{Ti}^+\text{Ar}_6$  symmetry is restored by forming a perfect octahedron with six equal Ti–Ar

distances of 2.84 Å. This observation leads to the conclusion that a saturation of bonding in the  $\text{Ti}^+$  cation is obtained for the first time with the formation of  $\text{Ti}^+\text{Ar}_6$ , implying an energetically optimal structure. Larger clusters are then formed by capping the eight triangular faces of the  $\text{Ti}^+\text{Ar}_6$  octahedron with Ar atoms, building thus a second solvation shell.

In the top of Fig. 3 we plot the binding energy of each  $\text{Ti}^+\text{Ar}_n$  cluster as a function of the cluster size  $n$ , and in the bottom of Fig. 3 we plot the binding energy differences,  $E(n) - E(n-1)$ , which are indicative of the stability of the clusters. These incremental binding energies show a local peak at  $n = 6$ , which also indicates the saturation of the bonding. Analysis of the molecular orbitals of the  $\text{Ti}^+\text{Ar}_n$  ( $n < 7$ ) clusters at the optimized geometry shows that the HOMOs involve an admixture of  $\text{Ti}^+$  3d and 4s atomic orbitals. Qualitatively, as one goes from smaller to larger systems, the  $\text{Ti}^+3d$  configuration becomes more pronounced in the molecular orbitals. In the particular case of  $\text{Ti}^+\text{Ar}_6$ , by inspecting the HOMO, we find a 4s to 3d promotion for the  $\text{Ti}^+$  orbitals. Calculations by imposing the  $3d^24s^1$  configuration in the  $\text{Ti}^+\text{Ar}_6$  complex resulted in a total energy 0.55 eV higher than in the  $3d^34s^0$  configura-

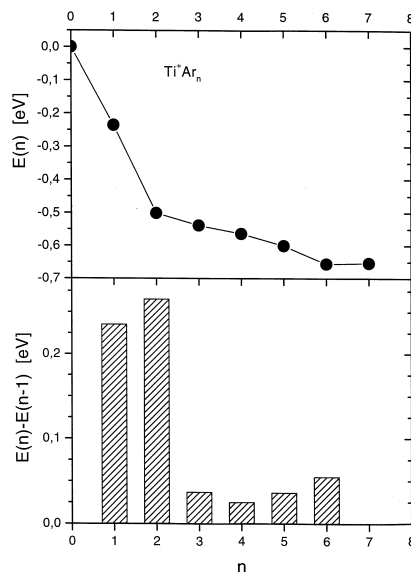


Fig. 3. Binding energies (top) and binding energy differences (bottom) for  $\text{Ti}^+\text{Ar}_n$  clusters.

tion. This indicates that a crossing between the two  $3d^24s^1$  and  $3d^34s^0$   $Ti^+$  states occurs in the  $Ti^+Ar_n$  clusters with  $1 < n < 6$ .

Assuming an electrostatic interaction for  $Ti^+-Ar$  the main contribution to the binding energy arises from the ion-induced dipole term  $q^2\alpha/(2R^4)$ , where  $q$  is the metal ion charge state and  $\alpha = 1.64 \text{ \AA}^3$  the Ar polarizability. At the equilibrium distance  $R = 2.65 \text{ \AA}$  for  $Ti^+Ar$  we obtain an interaction energy of 0.239 eV. This value is almost the same as that of the DFT calculation, suggesting that the interaction is mainly electrostatic. This indicates that the occupied  $Ti^+$  4s orbital plays the main role in the interaction of the diatomic complex. Otherwise, a complete 4s to 3d promotion would reduce the repulsion,

leading thus to a stronger binding as in the case of the  $Ni^+Ar$  complex [14] where the 4s orbital is unoccupied and the electrostatic energy at the equilibrium distance  $R = 2.42 \text{ \AA}$  is only  $\sim 75\%$  of the binding energy 0.456 eV. The longer equilibrium distance and the weaker interaction energy of  $Ti^+Ar$  in comparison to  $Ni^+Ar$  reflects the larger spatial extent of the 4s orbital of  $Ti^+$  in contrast to the more compact 3d orbital of  $Ni^+$ .

In Fig. 4, we present the three higher occupied molecular orbitals and the three first unoccupied orbitals of  $Ti^+Ar_6$ . The three occupied MOs are constructed from a linear combination of the  $d_{-1}$ ,  $d_{+1}$  and  $d_{-2}$  atomic orbitals of Ti with the p orbitals of the Ar atoms, respectively. The d orbitals of the

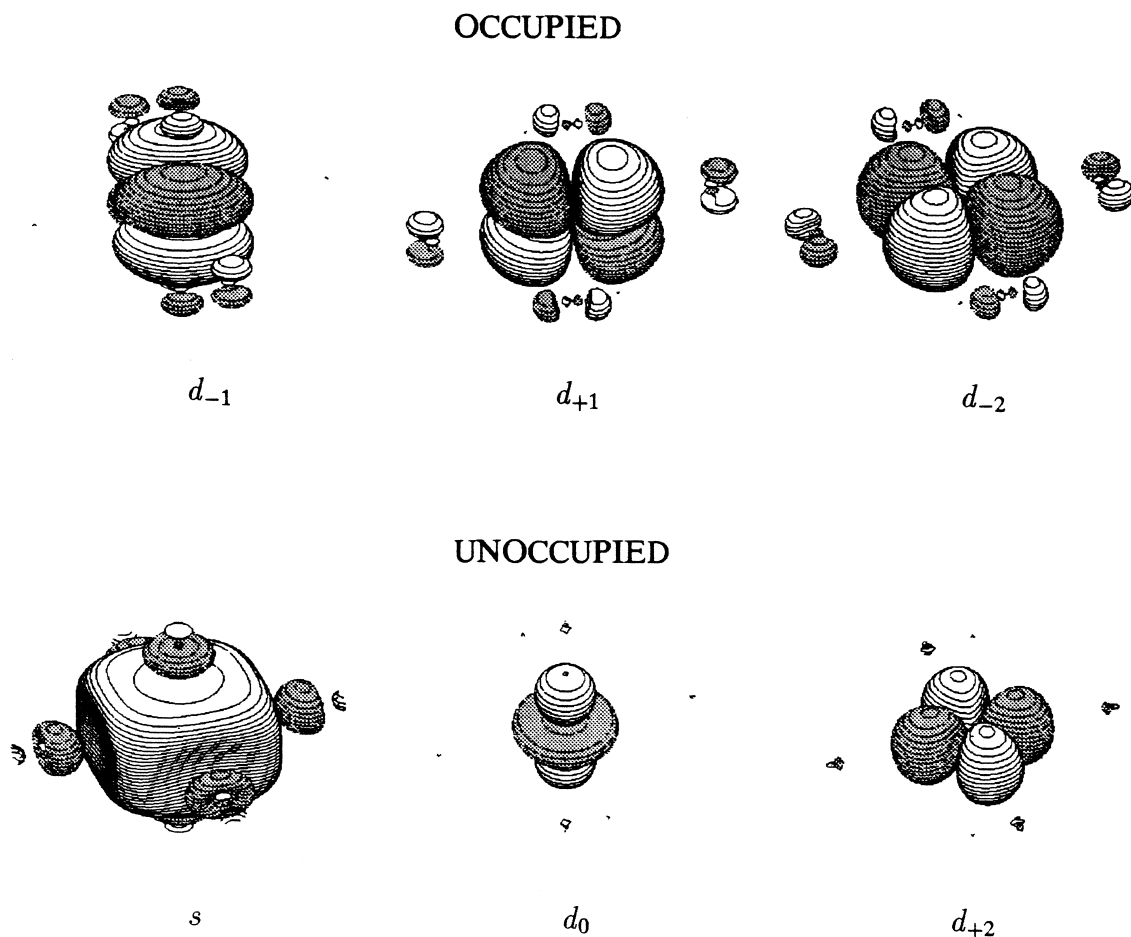


Fig. 4. The last three occupied molecular orbitals (top) and the first three unoccupied orbitals (bottom) of  $Ti^+Ar_6$ . The labels indicate the  $Ti^+$  orbitals involved in MOs (see text).

metal cation, which are involved in the HOMO are, in fact, the  $d_{xy}$ ,  $d_{yz}$  and  $d_{xz}$  components. These molecular orbitals are energetically degenerate and they are each occupied by one electron. The first three unoccupied molecular orbitals are linear combinations of the  $s$ ,  $d_0$  and  $d_{+2}$  atomic orbitals of Ti with the  $p$  orbitals of the Ar atoms. The  $d_0$  and  $d_{+2}$  atomic orbitals are the  $d_{z^2}$  and  $d_{x^2-y^2}$  real atomic orbitals, respectively.

From Fig. 4, it is evident that in the ground electronic state of the cluster the Ar atoms lie on the nodal planes of the Ti  $d$ -orbitals with the  $p$  orbitals perpendicular to them. Contrary to that, in the unoccupied orbitals (lower part of Fig. 4) we see that the Ar atoms are oriented towards the  $s$ ,  $d_0$  and  $d_{+2}$ , empty Ti atomic orbitals. This is in accord with a LFT description, which requires the five  $d$  orbitals of the metal to split into two degenerate sets, one with a three-fold degeneracy ( $d_{xy}$ ,  $d_{yz}$ ,  $d_{xz}$ ) and one with a two-fold degeneracy ( $d_{z^2}$ ,  $d_{x^2-y^2}$ ). Assuming electrostatic interactions among a metal cation with a  $3d^34s^0$  electronic configuration and six equivalent ligands, the latter will occupy the positions around the metal with the least electron repulsion. Thus, a perfect octahedral structure is formed for  $Ti^+Ar_6$ .

Octahedral arrangements were also observed for  $Rh^+Ar_6$  [12] and for  $Ti^+(H_2)_6$  [18]. Nevertheless, it is worth noting that studies on other ion-doped noble gas clusters, such as the  $C^+Ar_n$  [23],  $Ni^+Ar_n$  [14], and  $Nb^+Ar_n$  [12], have shown less symmetric coordination structures with only four strong bonds and two weak bonds. DFT type calculations are presumably only feasible at present for complexes of the size of  $Ti^+Ar_6$ . Although we cannot test the accuracy of these calculations with more elaborate theories, the minimum energy geometries which are predicted are in good agreement with the experimental observations.

#### 4. Conclusions

$Ti^+Ar_n$  clusters have been studied with a time-of-flight apparatus. The mass spectrum was dominated by one high-intensity line of  $Ti^+Ar_6$ , although clusters with up to 50 Ar atoms were recorded. Density functional theory calculations with the three-parameter hybrid functional of Becke and the

Lee–Yang–Parr correlation functional (B3LYP) were performed to reveal the most stable structures of complexes with  $n = 1-7$  Ar atoms. In clusters with  $n < 6$  Ar atoms, the minimum energy geometries show one strong  $Ti^+Ar$  bond and  $n - 1$  weaker bonds with the Ar atoms at longer distances from titanium. The  $Ti^+Ar_6$  complex forms a regular octahedron with  $Ti^+$  in the center and the six Ar atoms filling the first solvation shell. Larger clusters have the Ar atoms loosely bound in the second solvation shell. The calculations fully support the stability of  $Ti^+Ar_6$  and its enhanced intensity in the mass spectrum.

#### References

- [1] D.E. Lessen, R.L. Asher, P.J. Brucat, in: M.A. Duncan (Ed.), *Advances in Metal and Semiconductor Clusters*, vol. I, JAI Press, Greenwich, CT, 1993.
- [2] C.W. Bauschlicher Jr., H. Partridge, S.R. Langhoff, in: M.A. Duncan (Ed.), *Advances in Metal and Semiconductor Clusters*, vol. II, JAI Press, Greenwich, CT, 1994.
- [3] W.H. Breckenridge, C. Jouvret, B. Soep, in: M.A. Duncan (Ed.), *Advances in Metal and Semiconductor Clusters*, vol. III, JAI Press, Greenwich, CT, 1995.
- [4] M. Velegarakis, Ch. Lüder, *Chem. Phys. Lett.* 223 (1994) 139.
- [5] Ch. Lüder, M. Velegarakis, *J. Chem. Phys.* 105 (1996) 2167.
- [6] Ch. Lüder, D. Prekas, M. Velegarakis, *Laser Chem.* 17 (1997) 109.
- [7] D. Prekas, Ch. Lüder, M. Velegarakis, *J. Chem. Phys.* 108 (1998) 4450.
- [8] G.S. Fanourgakis, S.C. Farantos, *J. Phys. Chem.* 100 (1996) 3900.
- [9] G.S. Fanourgakis, S.C. Farantos, Ch. Lüder, M. Velegarakis, S.S. Xantheas, *J. Chem. Phys.* 109 (1998) 108.
- [10] D.E. Lessen, P.J. Brucat, *Chem. Phys. Lett.* 149 (1988) 10.
- [11] D.E. Lessen, P.J. Brucat, *Chem. Phys. Lett.* 91 (1989) 4522.
- [12] M. Beyer, C. Berg, G. Albert, U. Achatz, V.E. Bondybey, *Chem. Phys. Lett.* 280 (1997) 459.
- [13] S. Bililign, C.S. Feigerle, J.C. Miller, M. Velegarakis, *J. Chem. Phys.* 108 (1998) 6312.
- [14] M. Velegarakis, G.E. Froudakis, S.C. Farantos, *J. Chem. Phys.* 109 (1998) 4687.
- [15] H. Partridge, C.W. Bauschlicher Jr., S.R. Langhoff, *J. Phys. Chem.* 96 (1992) 5350.
- [16] H. Partridge, C.W. Bauschlicher Jr., *J. Phys. Chem.* 98 (1994) 2301.
- [17] P.A. van Koppen, P.R. Kemper, J.E. Bushnell, M.T. Bowers, *J. Am. Chem. Soc.* 117 (1995) 2098.
- [18] J.E. Bushnell, P. Maitre, P.R. Kemper, M.T. Bowers, *J. Chem. Phys.* 106 (1997) 10153.

- [19] L.B. Knight Jr., K.A. Keller, R.M. Babb, *J. Chem. Phys.* 105 (1996) 5331.
- [20] M.J. Frisch, G.W. Trucks, H.B. Schlegel, P.M.W. Gill, B.G. Johnson, M.A. Robb, J.R. Cheeseman, T. Keith, G.A. Petersson, J.A. Montgomery, K. Raghavachari, M.A. Al-Laham, V.G. Zakrzewski, J.V. Ortiz, J.B. Foresman, J. Cioslowski, B.B. Stefanov, A. Nanayakkara, M. Challacombe, C.Y. Peng, P.Y. Ayala, W. Chen, M.W. Wong, J.L. Andres, E.S. Replogle, R. Gomperts, R.L. Martin, D.J. Fox, J.S. Binkley, D.J. Defrees, J. Baker, J.P. Stewart, M. Head-Gordon, C. Gonzalez, J.A. Pople, *Gaussian 94*, Revision D.4, Gaussian, Inc., Pittsburgh, PA, 1995.
- [21] A.D. Becke, *J. Chem. Phys.* 98 (1993) 5648.
- [22] C. Lee, W. Yang, R.G. Parr, *Phys. Rev. B* 37 (1988) 785.
- [23] G.E. Froudakis, G.S. Fanourgakis, S.C. Farantos, S.S. Xanthreas, *Chem. Phys. Lett.* 294 (1998) 109.